Journal of Exposure Science and Environmental Epidemiology (2009), 1–10
© 2009 Nature Publishing Group All rights reserved 1559-0631/09/$32.00
www.nature.com/jes

Assessing exposure to granite countertops—part 2: Radon

JOSEPH G. ALLEN[a], TAEKO MINEGISHI[a], THEODORE A. MYATT[a], JAMES H. STEWART[a,b], JOHN F. MCCARTHY[a] AND DAVID L. MACINTOSH[a]

[a]*Environmental Health & Engineering, Needham, MA, USA*
[b]*Harvard School of Public Health, Department of Environmental Health, Boston, MA, USA*

Radon gas (^{222}Rn) is a natural constituent of the environment and a risk factor for lung cancer that we are exposed to as a result of radioactive decay of radium (^{226}Ra) in stone and soil. Granite countertops, in particular, have received recent media attention regarding their potential to emit radon. Radon flux was measured on 39 full slabs of granite from 27 different varieties to evaluate the potential for exposure and examine determinants of radon flux. Flux was measured at up to six pre-selected locations on each slab and also at areas identified as potentially enriched after a full-slab scan using a Geiger–Muller detector. Predicted indoor radon concentrations were estimated from the measured radon flux using the CONTAM indoor air quality model. Whole-slab average emissions ranged from less than limit of detection to 79.4 Bq/m^2/h (median 3.9 Bq/m^2/h), similar to the range reported in the literature for convenience samples of small granite pieces. Modeled indoor radon concentrations were less than the average outdoor radon concentration (14.8 Bq/m^3; 0.4 pCi/l) and average indoor radon concentrations (48 Bq/m^3; 1.3 pCi/l) found in the United States. Significant within-slab variability was observed for stones on the higher end of whole slab radon emissions, underscoring the limitations of drawing conclusions from discrete samples.
Journal of Exposure Science and Environmental Epidemiology advance online publication, 26 August 2009; doi:10.1038/jes.2009.43

Keywords: *radon, granite, countertops, exposure, indoor air.*

Introduction

Concrete, brick, gypsum, stone, and other structural building materials have long been recognized as a source of radon in residential and other buildings (Ingersoll, 1983; Mustonen, 1984; NCRP, 1987b; Stranden, 1988; Khan et al., 1992; Lee et al., 2001; Sahoo et al., 2007). Given their low emission rates of radon and the potential for entry of radon into occupied areas to be impeded by surface finishes (for example, paint and flooring), most structural building materials have been thought to make a negligible contribution to radon exposures inside a structure (NCRP, 1987a, b, 1993). However, with the increased use of natural stone as a functional and ornamental feature inside homes, such as a kitchen or bath countertop, it is important to determine whether these natural stones can be a meaningful source of radon in indoor environments.

These "stone" materials are typically referred to as "granite", but in fact can consist of a variety of rock-types that include granite and marble (hereafter collectively referred to as "granite"). Radon flux for these stones has been previously reported to range from 0.01 to 13.5 Bq/m^2/h among ~500 samples of structural and unidentified granite building materials obtained from several nations of Africa, Asia, and the Middle East (Khan et al., 1992; Chao and Tung, 1999; El-Dine et al., 2001; al-Jarallah, 2001; al-Jarallah et al., 2001, 2005; Petropoulos et al., 2002; Fazal ur et al., 2003; Stoulos et al., 2003; Sundar et al., 2003; Arafa, 2004; Osmanlioglu, 2006; Singh et al., 2008; Sonkawade et al., 2008). The extent to which the granite samples examined in those studies represent inventories of natural stone countertops has not been evaluated. Moreover, thorough exposure assessments of radon emissions from these types of stones were not conducted. Consequently, the potential for natural stone materials used as kitchen and bathroom countertops to be an important source of radon exposure in indoor air has not been assessed in a rigorous manner.

To address this knowledge gap, radon flux was determined for 39 full slabs of granite intended for sale as countertop material in the United States. As an installation of countertop typically includes most or all of a slab, estimates of the slab-average radon flux are a primary product of the investigation. Potential covariates of slab-average radon flux, such as surface condition of the slab, intra-slab variation of radon flux, and radium activity concentrations, were evaluated as predictors of radon emissions for possible use in future analyses. Indoor air concentrations of radon released from granite countertops inside a home were estimated from the measured fluxes used as input for a generally accepted

1. Address all correspondence to: Dr. Joseph G. Allen, Environmental Health & Engineering, 117 Fourth Avenue, Needham, MA 02494-2725, USA. Tel: +1 800 825 5343. Fax: +1 781 593 3862.
E-mail: jallen@eheinc.com
Received 8 April 2009; revised 20 June 2009; accepted 13 July 2009

Material may be protected by copyright law (Title 17, U.S. Code)

indoor air quality model. Finally, granite countertop-related radon exposure was characterized using normative data and guidance published by the US Environmental Protection Agency.

Methods

Overview

A total of 39 different slabs of natural stone intended for sale as granite countertops were evaluated, with at least one slab from each of 27 unique varieties of stone. Three slabs from each of six varieties of granite were analyzed to assess the variability that can exist across slabs of the same type. Along with assessing flux across granite varieties, the study design allowed for: assessment of intra-slab variability; comparison of full-slab evaluation *versus* discrete sampling; and identification of factors that may influence radon flux. Market share was determined from 1 year of the most recent sales data obtained from 13 of the largest suppliers of granite in the United States, representing nearly 800,000 sales of granite from 18 countries.

Testing was first conducted on intact, full slabs, with each slab measuring $\sim 3\,\text{m} \times 1.8\,\text{m} \times 3.2\,\text{cm}$. Radon flux was determined simultaneously at up to six evenly distributed and pre-determined locations selected using a standardized grid template. These measurements at pre-determined locations were supplemented by screening the entirety of each slab using a Geiger–Muller (GM) counter to identify potentially enriched areas defined as >500 counts per minute (c.p.m.) of radioactivity). A value of 500 c.p.m. was selected as the criteria for identifying potentially enriched areas based on pilot testing ($n = 757$), in which 99.6% of measurements were <250 c.p.m., and only 3 measurements were >500 c.p.m. Flux measurements were also obtained at these potentially enriched areas. During all sampling events for radon flux, slabs were placed in a horizontal position across supports ~ 1 m above the ground. The supports only made contact with a limited area of the slabs, which enabled free flow of air underneath the slab. Seven of the slabs were selected for additional testing to characterize radon emissions from the unpolished, bottom surface of the granite. Two small pieces 6.5 cm × 13 cm were then cut from opposite ends of each slab and measured for radon flux to determine whether discrete samples could be a useful predictor of whole-slab radon emissions.

Radon Flux Measurements

For intact, full-slab sampling, radon flux was measured at each site using a flux chamber connected to a real-time radon monitor with a rapid response time (Durridge Rad-7 Radon Monitors, Bedford, MS, USA). The radon monitor has a reported accuracy range of ±5%, and the reported precision is ±54% at 37 Bq/m^3 (1 pCi/l) and ±12% at 740 Bq/m^3 (20 pCi/l) for 1-h average measurements. The radon monitor was purged for at least 10 min before beginning a test. For each test, the flux chamber (volume of 0.0016 cubic meters (m^3) and surface area of 0.038 square meters (m^2)) was fit to a rubber gasket, placed on the granite surface at the pre-specified location, and weighted with 0.9 kg (2 pounds) to seal the gasket against the surface. The monitor and tubing added an additional 0.0013 m^3 to the flux chamber setup, bringing the total volume to 0.003 m^3. The radon monitor drew and returned air at a flow rate of 0.7 l/min, resulting in constant air pressure in the flux chamber. Air from the flux chamber was passed through a desiccation column to remove any moisture.

One-hour integrated radon concentrations were recorded every hour, for a minimum of 24 h. These measurements were subsequently characterized as follows:

$$C_t = C_{\text{sat}}(1 - e^{-kt}) \tag{1}$$

where C_t is the 1-h average radon concentration at time t (Bq/m^3), C_{sat} is the saturated radon concentration (Bq/m^3), k is total instantaneous loss rate for radon (per h), and t is the elapsed time (h). In this equation, k is the sum of loss by radioactive decay of radon, diffusion through the slab, and any leakage between the sampling system and the granite slab. The parameters C_{sat} and k were estimated from equations (1) using an iterative curve-fitting method implemented with the NLIN procedure in SAS statistical software (SAS Institute, Cary, NC, USA).

Radon flux was then calculated using the estimate of C_{sat} and k, based on the following equation:

$$F = \frac{C_{\text{sat}} \times V \times k}{A} \tag{2}$$

where F is the flux (Bq/m^2/h), V is the total volume of sampling system (m^3), and A is the surface area under the flux chamber (m^2).

For granite slabs that had potentially enriched areas identified using the GM (3 out of 27 granite varieties), slab-average flux was calculated using a weighted average approach based on the percent of surface area represented by each test chamber. For the remaining stones, slab-average flux was calculated as the average of the results for the six pre-determined locations.

For the discrete sample testing, two pieces obtained from the corners of each slab were measured for radon flux (denoted C1 and C2). Each 6.5 cm × 13 cm sample was separately placed inside the flux chamber described above and the bottom of the chamber was sealed against an impermeable aluminum membrane. All flux calculations were conducted in the same manner as for the full-slab surface testing. In addition to the flux measurements, the radium-226 (^{226}Ra) activity of each corner sample was measured using gamma spectroscopy with a high-purity germanium detector, the details of which are described in Myatt et al. (2009).

Material may be protected by copyright law (Title 17, U.S. Code)

Exposure Modeling

The CONTAM multi-zone indoor air quality model (Walton and Dols, 2003) developed by the National Institute of Standards and Technology (NIST) was used to estimate indoor radon concentrations following a previously published methodology (Myatt et al., 2008; MacIntosh et al., 2009). Briefly, airflow among indoor and outdoor zones of the building (that is, rooms and ambient air) in CONTAM occurs through flow paths such as doors, windows, and cracks. The empirical power law relationship between airflow and pressure differences across a flow path is used to calculate inter-zonal flow in the model. Airflow between indoor zones induced by a recirculating, forced air heating and cooling system can also be simulated with CONTAM. Once airflows among zones are established, pollutant concentrations based on sources and sinks in each zone are calculated using mass balance equations.

The model was run under four scenarios—two home ventilation conditions (natural ventilation and forced air heating and cooling) for each of two residential building templates developed by NIST. The home templates represent a post-1990, two-story detached home and a pre-1940, single-story detached home (Table 1). An important variable in modeling expected indoor air contaminant concentrations is the home ventilation rate, typically measured as air changes per hour (ACH). Air exchange rates in residential buildings vary based on the type of construction, variability in weather, and geographic region (ASHRAE, 2005). Typical air exchange rates for residential buildings in North America range from a seasonal average of about 0.2 ACH for tightly constructed homes to upward of 2 ACH for loosely constructed housing (ASHRAE, 2005). Additional studies have shown that an ACH of ~ 0.5 is a reasonable estimate of average seasonal air exchange rate for residences (Grimsrud et al., 1982; Palmiter and Brown, 1989; Ek et al., 1990; Parker et al., 1990). The low end of the range, 0.2 ACH, was used as the annual average ACH for the naturally ventilated newer home scenario and the average of 0.5 ACH was used for the naturally ventilated older home scenario.

A radon flux of 1 $Bq/m^2/h$ and the surface area parameters identified in Table 1 were used to perform unit emission model runs with CONTAM. Results from the unit emission model runs were then scaled to represent the full range of radon flux values measured in this study. The modeling results are summarized on a whole-house average and room average basis for each residential scenario to characterize the variation of estimated countertop-related indoor radon among and within homes. In addition, the average of the four residential scenarios is reported for the slab-average flux of each granite type included in this study to provide an estimate of the potential slab-specific contribution to indoor radon.

Sales data of 2 months obtained from a natural stone supplier were used to estimate the surface area of granite countertop in homes. The average installation calculated from these data consisted of 4.7 m^2 (50 ft^2) and 1.7 m^2 (18 ft^2) of granite countertop in kitchens and bathrooms, respectively. Countertop allocated to bathrooms was divided among the bathrooms in each template. The total footprint of 6.4 m^2 (68 ft^2) was extrapolated to an overall surface area for radon flux of ~ 13.4 m^2 (144 ft^2) accounting for potential emissions from the top, bottom, and edges of the countertop.

Statistical Analysis

Statistical analyses were performed using SAS Statistical Software (SAS 9.1.3 Service Pack 4; SAS Institute), and include summary descriptive statistics, Wilcoxon Signed-Rank Sum tests, Spearman rank correlations, linear regression, and linear mixed effects models. In regression models, outcome variables were natural log-transformed to satisfy normality assumptions. Non-linear curve fitting used to estimate k and C_{sat} was performed with initial parameters of 1.27 and 0.06, respectively. Statistical significance was defined at the $\alpha = 0.05$ level.

Quality Assurance

Quality assurance samples were obtained in the field throughout the period when radon flux measurements were made. Repeated measurements were made on alternate sampling days from a location on a single slab with relatively low radon flux (average of 3.8 $Bq/m^2/h$) to provide continuing calibration and to establish the method limit of detection (LOD). The LOD was 0.8 $Bq/m^2/h$, calculated as three times the standard deviation of repeated testing on the control sample. In addition, radon concentrations in air of the test room were measured on alternate days to control for potential variation in background levels of radon. The average indoor radon concentration during the sampling period was 37 Bq/m^3 (1 pCi/l), similar to the median indoor radon concentration for the United States (Marcinowski

Table 1. Characteristics used to estimate indoor air radon concentrations for homes with natural ventilation and forced air central air conditioning

CONTAM Template	Age	Air exchange rate per hour		No. of floors	Home surface area, m^2 (ft^2)			No. of bath	Countertop surface area, m^2 (ft^2)	
		Natural	(Forced air)		Home	Kitchen	Bathroom		Kitchen	Bathroom
DH72	Before 1940	0.5	0.4	1	177 (1900)	28 (300)	18.6 (200)	2	4.7 (50)	1.7 (18)
DH28	After 1990	0.2	0.2	2	279 (3000)	18.6 (200)	34.4 (370)	3.5	4.7 (50)	1.7 (18)

Material may be protected by copyright law (Title 17, U.S. Code)

et al., 1994). Sampling devices were rotated between field tests and quality assurance tests to limit any potential instrument bias.

A three-phase diagnostic test was used to quality assure the estimates of C_{sat} and k obtained from the curve-fitting procedure: (1) data points were plotted with the corresponding best-fit curve and visually inspected for anomalies or outliers, (2) final flux chamber concentrations had to exceed 74 Bq/m^3 (2.0 pCi/l) (which is approximately four times the sensitivity of the instrument), and (3) model R^2 values had to be greater than 0.40. Samples failing any of these criteria were determined to be less than LOD and assigned a value of $\frac{1}{2}$ LOD for statistical analyses. Emission rates were not blank corrected for purposes of estimating slab-average flux and indoor radon levels.

Results

Radon Flux Measurements

Summary statistics for radon flux measurements from the 39 granite slabs (27 unique varieties) are shown in Table 2, with results presented in order of decreasing market share. Results are shown separately for measurements taken on the top or bottom of the stone, whether or not the bottom had a fiberglass backing, and whether the measurements occurred at pre-defined sampling locations ("Grid") or potentially enriched areas identified with the GM ("Off-Grid"). Slab-average radon flux ranged from <0.8 to 79 Bq/m^2/h, with a median of 3.9 Bq/m^2/h (average 9.6 Bq/m^2/h). The maximum flux value for any single sample was 1,300 Bq/m^2/h. For the slab with the maximum value (stone no. 24), the small area represented by the maximum flux combined with very low emissions from the bottom of the slab indicate a full-slab emission rate of 79 Bq/m^2/h.

Of the seven granite slabs selected to characterize radon emissions from the unpolished, bottom surface of the granite, two had fiberglass mesh backing on the bottom surface, a material and technique that is commonly used to provide structural support to a slab. Radon emissions from bottom surfaces with backings were up to three orders of magnitude lower than the top surface, even though these two slabs were on the high end of the distribution for radon emissions on the top surface (Table 2). The results of a paired analysis between the polished and unpolished surface (Wilcoxon Signed-Rank Sum test) for the five granite slabs that did not have the fiberglass mesh backing indicate that radon emissions from the unpolished surface were similar to the polished surface, on average (difference 0.1–6.0 Bq/m^2/h; $P=0.76$; $n=5$).

The slab-average radon emission results in Table 2 incorporate flux values from the underside when measured. For several slabs that had backing on the underside but no corresponding measurements, the expectation is that the side with backing would have significantly reduced radon emissions. However, as we did not have measurements to confirm this effect for all slabs with backing, the results presented did not have any correction applied and are presumed to provide an overestimate of emissions.

There was a strong, positive relationship between slab-average radon flux and within-slab variability (Spearman $r=0.96$; $P<0.01$) (that is, slabs at the higher end of radon flux exhibited the greatest within-slab variability) (Figure 1a). For one slab at the higher end of radon emissions, the difference between the minimum and maximum flux measurements spanned three orders of magnitude, whereas several slabs at the lower end of emissions had all measurements less than the detection limit. Similarly, comparing slabs of the same color (six types), slabs at the higher end of radon emissions exhibited greater within slab variability than those at the lower end.

Radon flux from discrete corner samples (C1 and C2) is also presented in Table 2. Radon flux for the two corner samples obtained from each slab were significantly correlated (Spearman $r=0.64$; $P<0.01$), although flux differed by approximately a factor of 10 for seven pairs of corner samples. C1 and C2 samples were independent significant predictors of log-transformed slab-average flux in linear regression analyses ($P<0.01$). The slopes from the models suggest a two unit increase in slab-average flux for every unit increase in discrete sample flux, on average, yet for some samples, the discrete samples are 10-fold higher than slab-average flux. This general lack of predictability is evidenced by the R^2 values from the models, which indicate that the discrete corner samples explain a relatively small amount of variability in slab-average flux ($R^2=0.32$ (C1); 0.23 (C2)).

As expected, radium content, measured in Bq/kg (Myatt et al., 2009), from the discrete corner samples was significantly associated with radon flux from the same samples (Spearman $r=0.76$; $P<0.01$) (Figure 2). Additionally, in linear regression analyses, ^{226}Ra activity measured in the corner samples was a significant predictor of slab-average flux, on average ($P<0.01$), yet the model R^2 values were moderately low ($R^2=0.41$ (C1); 0.38 (C2)).

Predicted Contribution to Indoor Radon

The predicted whole-house average radon concentrations for the four scenarios (old and new home, with both run under two ventilation rate conditions) are all <15.2 Bq/m^3 (0.4 pCi/l) for the full range of slab-average radon fluxes presented in Table 2. The newer home (template DH28) had higher predicted radon concentrations compared with the older home (template DH72), which can be explained by the lower ACH in the newer home (0.2 ACH *versus* 0.4–0.5 ACH).

Results for the newer home (template DH28) under the natural ventilation scenario are presented in Figure 3.

Material may be protected by copyright law (Title 17, U.S. Code)

Table 2. Summary statistics for radon flux (Bq/m^3) for measurements made on each slab by back mesh (presence of a fiberglass mesh backing), side (top or bottom), location (grid or off-grid), and for measurements made on each corner sample (C1 and C2), presented in order of decreasing market share.

Granite color no	% Market share	Granite name	Back mesh	Side	Location	*N*	Mean	Std dev	Min	Median	Max	Slab avg	C1	C2
1	5.4	Giallo Santa Cecilia	N	Top	Grid	6	<LOD	NA	<LOD	<LOD	<LOD	<LOD	<LOD	<LOD
2	5.4	New Venetian Gold	N	Top	Grid	6	1.7	0.42	1.1	1.7	2.2	1.7	3.9	<LOD
3	2.9	Tropical Brown	N	Top	Grid	6	3.0	0.43	2.4	3.0	3.6	3.0	1.9	1.6
4	2.5	Tan Brown	N	Top	Grid	6	<LOD	NA	<LOD	<LOD	<LOD	<LOD	<LOD	<LOD
5	2.1	Baltic Brown	N	Top	Grid	6	1.8	0.20	1.6	1.8	2.1	2.6	1.5	0.95
				Bottom	Grid	6	3.4	0.26	2.9	3.5	3.7	–	–	–
		Baltic Brown 2	N	Top	Grid	6	3.9	0.52	3.3	3.8	4.6	3.9	1.9	0.97
		Baltic Brown 3	N	Top	Grid	6	3.3	0.29	2.9	3.3	3.8	3.3	1.1	0.95
6	2.1	Giallo Veneziano	N	Top	Grid	6	0.48	0.18	<LOD	<LOD	0.85	<LOD	<LOD	<LOD
7	1.5	Green Butterfly	N	Top	Grid	4	<LOD	NA	<LOD	<LOD	<LOD	<LOD	<LOD	<LOD
8	1.2	Galaxy Black	N	Top	Grid	3	<LOD	NA	<LOD	<LOD	<LOD	<LOD	<LOD	<LOD
9	1.1	Blue Pearl	N	Top	Grid	6	<LOD	NA	<LOD	<LOD	<LOD	<LOD	<LOD	<LOD
				Bottom	Grid	6	0.51	0.24	<LOD	<LOD	1.0	–	–	–
		Blue Pearl 2	N	Top	Grid	6	<LOD	NA	<LOD	<LOD	<LOD	<LOD	<LOD	<LOD
		Blue Pearl 3	N	Top	Grid	6	<LOD	NA	<LOD	<LOD	<LOD	<LOD	<LOD	<LOD
10	1.1	Madurai Gold	N	Top	Grid	6	0.57	0.40	<LOD	<LOD	1.4	<LOD	<LOD	1.3
11	1.0	Crema Bordeaux	Y	Top	Grid	6	12	4.8	6.8	12	18	12	1.2	2.1
12	0.6	Giallo Vyara	N	Top	Grid	3	1.1	0.20	1.0	1.1	1.3	1.1	<LOD	<LOD
13	0.5	Shivakashi	N	Top	Grid	4	14	15	3.8	7.9	35	14	24	28
14	0.5	Copper Canyon	Y	Top	Grid	3	<LOD	NA	<LOD	<LOD	<LOD	<LOD	<LOD	<LOD
15	0.5	Juparana Persa	N	Top	Grid	5	2.0	0.98	1.0	1.9	3.6	2.0	0.92	0.90
16	0.5	Delicatus	Y	Top	Grid	6	0.57	0.24	<LOD	<LOD	0.88	0.57	0.40	<LOD
17	0.5	Juparana Bordeaux	Y	Top	Grid	6	81	22	58	80	120	41	16	19
				Bottom	Grid	5	0.97	1.2	<LOD	<LOD	3.2	–	–	–
18	0.4	Crystal Gold	N	Top	Grid	5	5.2	0.27	4.8	5.3	5.5	5.2	3.1	3.6
19	0.4	Golden River	Y	Top	Grid	6	4.5	1.8	2.6	4.1	7.5	4.5	2.6	<LOD
20	0.4	Mascarello	Y	Top	Grid	5	27	22	3.6	23	63	27	9.1	1.3
21	0.3	Golden Typhoon	Y	Top	Grid	6	4.7	1.5	2.7	4.5	6.9	4.7	2.4	1.9
22	0.3	Arandis	N	Top	Grid	6	11	3.4	6.8	10	17	11	8.5	11
23	0.2	Namibian Gold	N	Top	Grid	4	4.5	1.7	2.1	4.9	6.2	7.4	4.1	0.86
					Off-Grid	2	24	18	11	24	36	–	–	–
				Bottom	Grid	5	5.6	3.0	3.3	4.2	11	–	–	–
					Off-Grid	1	25	NA	25	25	25	–	–	–
		Namibian Gold 2	N	Top	Grid	3	4.5	1.8	3.0	4.0	6.5	4.4	14	0.83
					Off-Grid	1	3.1	NA	3.1	3.1	3.1			
		Namibian Gold 3	N	Top	Grid	6	3.4	1.7	1.4	3.2	6.0	3.4	1.3	9.2
24	0.2	Nile Gold	Y	Top	Grid	6	32	67	2.2	3.6	170	79	2.4	1.0
					Off-Grid	3	1200	150	1000	1200	1300	–	–	–
				Bottom	Grid	4	3.8	6.2	<LOD	0.79	13	–	–	–
					Off-Grid	2	2.4	1.5	1.3	2.4	3.5	–	–	–
		Nile Gold 2	N	Top	Grid	3	26	22	8.4	18	51	27	29	5.3
					Off-Grid	3	34	13	22	35	47	–	–	–

Material may be protected by copyright law (Title 17, U.S. Code)

Table 2. *Continued*

Granite color no	% Market share	Granite name	Back mesh	Side	Location	N	Mean	Std dev	Min	Median	Max	Slab avg	C1	C2
		Nile Gold 3	N	Top	Grid	4	5.3	6.0	1.5	2.6	14	29	4.9	–
					Off-Grid	5	120	74	22	100	210	–	–	–
25	0.2	Kashmir Gold	N	Top	Grid	6	4.4	1.0	3.2	4.2	6.0	5.2	1.8	1.7
				Bottom	Grid	6	5.9	1.5	4.1	6.0	8.1	–	–	–
		Kashmir Gold 2	N	Top	Grid	6	23	12	8.3	21	44	23	3.1	30
		Kashmir Gold 3	N	Top	Grid	6	27	12	13	26	48	27	12	14
26	0.2	Golden Peach	N	Top	Grid	4	1.8	0.31	1.5	1.8	2.2	1.8	0.97	0.95
27	<0.01	Shiva Pink	N	Top	Grid	6	5.4	2.1	2.1	5.5	8.5	5.5	2.6	3.0
				Bottom	Grid	4	5.7	2.4	3.0	5.5	8.8	–	–	–
		Shiva Pink 2	N	Top	Grid	6	4.8	2.0	3.4	4.2	8.6	4.8	13	1.4
		Shiva Pink 3	N	Top	Grid	5	9.8	5.6	4.0	7.6	16	13	3.3	2.7
					Off-Grid	1	57	NA	57	57	57	–	–	–

Estimated radon concentrations in the source rooms (kitchen, bathroom) were higher than the corresponding whole-house concentrations, although the degree of between-room variation was muted for the forced air ventilation scenario because the central fan and supply air distribution system provided a relatively homogeneous distribution of radon throughout the home. Although kitchen concentrations are higher in the naturally ventilated home, the forced air ventilation scenario actually yielded higher whole-house radon concentration estimates owing to a more uniform distribution of air throughout the home.

Measured radon flux from this study, predicted indoor radon concentration, market share data, and radon reference values are presented in Figure 4. The six granite types for which radon flux was measured from three slabs are denoted with an asterisk (*) in Figure 4. The variability observed among the triplicate slabs is depicted, with bars showing the range in slab-average radon emissions. The granite types that constitute the majority of slabs sold are on the lower end of radon emissions and exhibit the least variability. Granite types on the higher end of radon emissions generally exhibited greater variability and account for <1% of the market share.

Discussion

Slab-average radon flux observed in this study was similar to radon emissions reported previously for samples of granite building materials. In 14 peer-reviewed studies representing over 500 granite samples collected around the world, radon flux ranged from 0.01 to 13.5 Bq/m^2/h (Khan et al., 1992; Chao and Tung, 1999; El-Dine et al., 2001; al-Jarallah, 2001; al-Jarallah et al., 2001, 2005; Petropoulos et al., 2002; Fazal ur et al., 2003; Stoulos et al., 2003; Sundar et al., 2003; Arafa, 2004; Osmanlioglu, 2006; Singh et al., 2008; Sonkawade et al., 2008). In comparison, we found slab-average radon flux of <0.8–79 Bq/m^2/h. The previously published reports do not include detailed information on the types of granite that were evaluated, thus those flux measurements cannot be linked to specific types of granite sold as countertop. Moreover, descriptions contained in these papers indicate that the samples include granite intended for uses other than countertops in residences. Nonetheless, radon emission characteristics of the countertop slabs included in this study and the granite samples reported in other reports seem to be similar.

Some of the slabs in our study exhibited a substantial amount of spatial variability in radon flux, as indicated by the modest strength of the association between radon flux found for (1) multiple locations on a single slab; (2) corner samples of the same stone; and (3) individual sample results and estimates of slab-average flux as well as the effect of surface conditions such as polishing and fiberglass mesh

Material may be protected by copyright law (Title 17, U.S. Code)

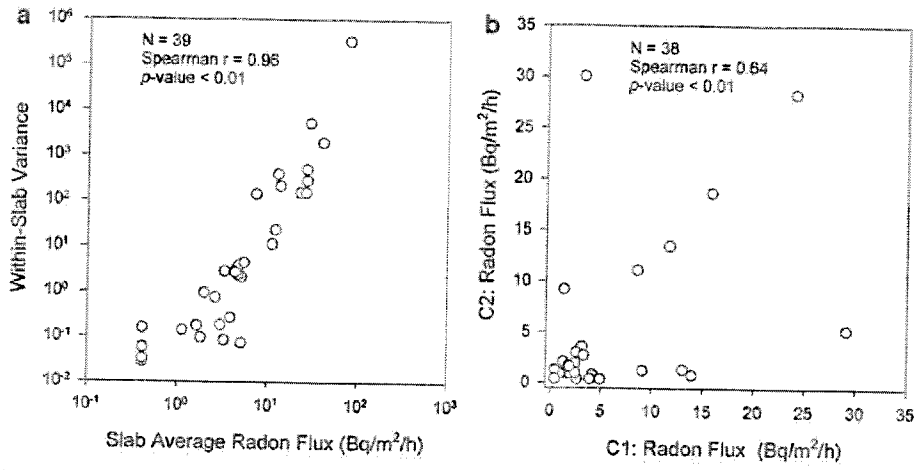

Figure 1. Relationship between slab-average radon flux and within-slab variance (a), and radon flux measured from corner pieces (C1 + C2) from the same slab (b).

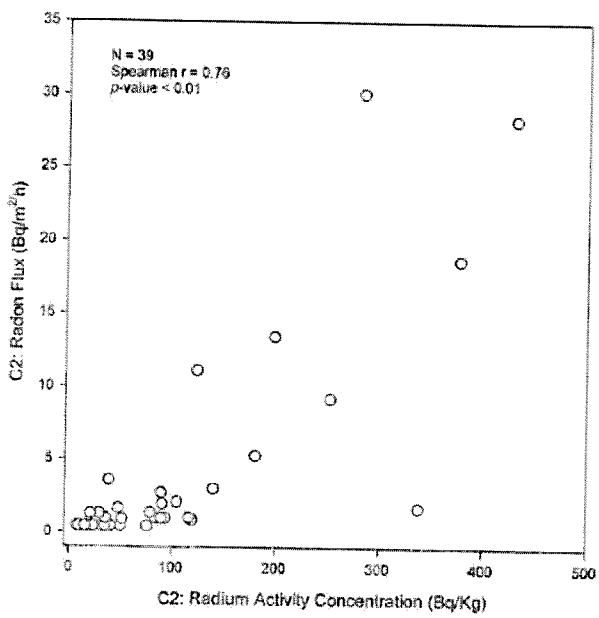

Figure 2. Relationship of radium activity concentration (Bq/kg) and radon flux (Bq/m^2/h) in one set of corner samples.

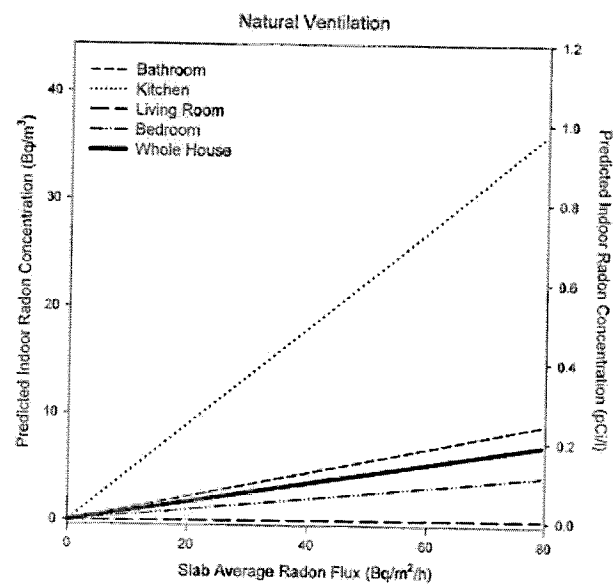

Figure 3. Whole-house and room-specific predicted indoor radon concentrations in a model home under a natural ventilation scenario.

backing. The strong concordance observed between the ^{226}Ra-series activity and radon flux in the corner samples indicates that the intra-slab variation of radon flux reflects heterogeneity of ^{226}Ra concentrations in the stone.

Intra-slab variation of radon flux could also be influenced by the concentration gradient in the flux chamber, and any corresponding back diffusion through the slab. This effect would manifest as a difference in the overall loss rate (k), estimated using the curve-fitting method between locations with high and low flux. However, we found no significant association between k and flux (linear mixed effects model; $P = 0.56$), which suggests that differences in back diffusion among test locations are not an important contributor to the intra-slab variation in radon flux that was observed.

Variability of radon flux within a slab was also found to be influenced by the presence of fiberglass mesh backing that was present on some of the stones. Radon emissions from the side with backing were up to three orders of magnitude lower than the polished side intended to be the top surface of the counter. Measurements taken on a countertop surface without accounting for backing material on the underside

Material may be protected by copyright law (Title 17, U.S. Code)

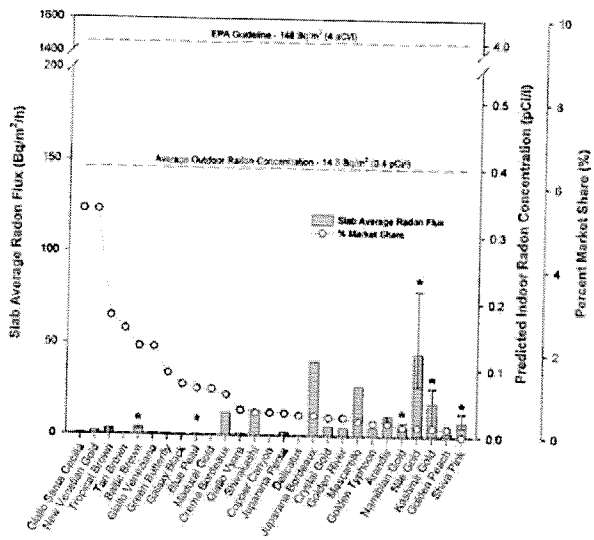

Figure 4. Radon flux measurements of full slabs and predicted contribution to indoor radon concentrations by granite type, in order of decreasing market share. Bars denoted with star (*) represent the range of test results from three slabs of that granite type.

could potentially lead to incorrect conclusions regarding full-slab radon emissions. Additional testing would be required to determine whether mesh backing helps mitigate the overall flux of radon from granite countertops. Emission rates were observed to be similar on the unpolished side of a slab for slabs without backing. Further research would need to be conducted to verify whether emission rates could vary between the two surfaces, perhaps as a result of differences in surface area and porosity caused by the polishing process.

The extent of within-slab variation in radon flux indicates that exposure assessments for granite countertop-related radon need to consider the full slab rather than spot measurements. Reliance on an elevated flux or radium measurement from a small sample may lead to an erroneous conclusion that the entire slab will make an important contribution to radon emissions (conversely, a low measurement on a localized area may lead to a conclusion that the entire slab is low emitting). This finding underscores the importance of full-slab evaluations, particularly for higher-emitting slabs, which showed increased intra-slab variability.

Testing of multiple locations and sides of a slab and calculation of slab-average radon flux as described here is one possible approach for evaluating granite countertop materials on a whole-slab basis. The requirement of numerous detailed measurements and the possibility of selecting locations that are not representative of total slab emissions of radon are limitations of this approach. Whole-slab testing in large-scale environmental chambers could also be employed to characterize radon flux from an entire slab. We found good agreement between the predicted indoor radon concentration determined from whole-slab radon flux characterized using the grid sampling approach in this study (2.1 Bq/m^3; 0.056 pCi/l) and a full-chamber test (1.2 Bq/m^3; 0.033 pCi/l) applied to a granite countertop that was cut and finished for use in a home. In addition to these methods, portal screening devices for the ^{226}Ra-series, possibly similar to the detectors used at points of entry in airports and other sensitive locations, could also be effective for obtaining estimates of whole-slab radon flux.

Estimated Indoor Radon Concentrations

The majority (82%) of granite slabs tested in this study have radon emissions that correspond to predicted indoor radon concentrations <1.9 Bq/m^3 (0.05 pCi/l). For the highest emitting slab in a tightly constructed house (worst case analysis for this study), the predicted whole-house annual average radon concentration is <11.1 Bq/m^3 (0.3 pCi/l). To characterize exposure to radon in indoor air of residences as a result of emissions from granite countertops, indoor air concentrations estimated from the measured radon flux can be compared with relevant benchmarks that include: (1) radon contributions from other sources in the home, (2) exposure guidelines for radon, and (3) background levels of radon.

Information on radon emissions was compiled for concrete, gypsum, and brick reported in the scientific literature to facilitate a comparison with emissions from granite countertops observed in this study. The average radon emissions for gypsum and concrete are 4 Bq/m^2/h and 8 Bq/m^2/h, respectively, calculated based on over 300 measurements of these common building materials (Ingersoll, 1983; Mustonen, 1984; Chao and Tung, 1999; Petropoulos et al., 2002; Stoulos et al., 2003; Maged and Ashraf, 2005; de Jong et al., 2006; Kobeissi et al., 2008; Ngachin et al., 2008; Sonkawade et al., 2008). Although the average radon emission rates for these building materials are similar to granite measured in this study (3.9 Bq/m^2/h) and in the scientific literature (1 Bq/m^2/h; 15 studies cited in the first paragraph of the Discussion), it is important to consider the mass of material in a home that may be emitting radon. A typical surface area potentially emitting radon for a granite countertop is 13 m^2 (144 ft^2), whereas that surface area may be 40 times higher for gypsum (550 m^2), and 10 times higher for concrete (140 m^2). These data suggest that emissions of radon from granite countertops may be a minor fraction of total radon emissions from building materials for a home constructed of concrete or gypsum board walls.

The US Environmental Protection Agency has established an action level of 148 Bq/m^3 (4.0 pCi/l) for radon in residential indoor air (US EPA, 1993). Similarly, the ICRP recommends an action level for radon in indoor air of dwellings that is no lower than 200 Bq/m^3 (5.4 pCi/l) (ICRP, 2005). In specific reference to building materials and radon,

Material may be protected by copyright law (Title 17, U.S. Code)

the EC states that the amount of radium in building materials should be below a level where it is likely to be a major contributor to radon concentrations in indoor air that exceed 200 Bq/m^3 (5.4 pCi/l) (European Commission, 1999). The market-share-weighted average concentration of radon in indoor air attributable to emissions from granite countertops measured in this study was estimated to be ~0.3 Bq/m^3 (0.009 pCi/l), ~400 times lower than the action level recommended by the EPA. However, a limitation of this analysis is that the stones from this study represent ~30% of market share. The indoor radon concentration estimated for the highest emitting stone (11.1 Bq/m^3; 0.3 pCi/l), is approximately one-tenth of the US Environmental Protection Agency action level of 148 Bq/m^3 (4.0 pCi/l), one-fourth of the average concentration of radon in indoor air of US homes (48 Bq/m^3; 1.3 pCi/l) (Marcinowski et al., 1994), and about equal to the average outdoor radon concentration in the US of 14.8 Bq/m^3 (0.4 pCi/l) (NCRP, 1987b).

Acknowledgements

Funding for this research was provided by the Marble Institute of America, Cleveland, OH, and the Environmental Health and Engineering, Needham, MA. We thank John D. Spengler, Ph.D., Akira Yamaguchi Professor of Environmental Health and Human Habitation, Harvard School of Public Health, Helen H. Suh, Sc.D., Associate Professor of Environmental Chemistry and Exposure Assessment, Harvard School of Public Health, and Brian J. Baker, Senior Engineer, EH&E, for their contributions.

References

al-Jarallah M. Radon exhalation from granites used in Saudi Arabia. *J Environ Radioact* 2001: 53(1): 91–98.

al-Jarallah M.I., Abu-Jarad F., and Fazal-ur-Rehman Determination of radon exhalation rates from tiles using active and passive techniques. *Radiat Meas* 2001: 34: 491–495.

al-Jarallah M.I., Fazal-ur-Rehman, Musazay M.S., and Aksoy A. Correlation between radon exhalation and radium content in granite samples used as construction material in SaudiArabia. *Radiat Meas* 2005: 40: 625–629.

Arafa W. Specific activity and hazards of granite samples collected from the Eastern Desert of Egypt. *J Environ Radioact* 2004: 75(3): 315–327.

ASHRAE. *2005 ASHRAE Handbook—Fundamentals [SI Edition]*. American Society of Heating, Refrigerating, and Air-Conditioning Engineers, Atlanta, GA, USA, 2005.

Chao C.Y., and Tung T.C. Radon emanation of building material–impact of back diffusion and difference between one-dimensional and three-dimensional tests. *Health Phys* 1999: 76(6): 675–681.

de Jong P., van Dijk W., van der Graaf E.R., and de Groot T.J. National survey on the natural radioactivity and ^{222}Rn exhalation rate of building materials in The Netherlands. *Health Phys* 2006: 91(3): 200–210.

Ek C.W., Onisko S.A., and Gregg G.O. Air leakage tests of manufactured housing in the Northwest United States. In: Sherman M.H. (Ed.). *Air Change Rate and Airtightness in Buildings, ASTM STP 1067*. American Society for Testing and Materials, Philadelphia, PA, USA, 1990, pp. 152–164.

El-Dine N.W., El-Shershaby A., Ahmed F., and Abdel-Haleem A.S. Measurement of radioactivity and radon exhalation rate in different kinds of marbles and granites. *Appl Radiat Isot* 2001: 55(6): 853–860.

European Commission . In: European Commission. Directorate-General - Environment Nuclear Safety and Civil Protection (Ed.). *Radiation Protection 112: Radiological Protection Principles Concerning The Natural Radioactivity Of Building Materials*. European Commission, 1999: Finland.

Fazal ur R., Al-Jarallah M.I., Musazay M.S., and Abu-Jarad F. Application of the can technique and radon gas analyzer for radon exhalation measurements. *Appl Radiat Isot* 2003: 59(5–6): 353–358.

Grimsrud D.T., Modera M.P., and Sherman M.H. A predictive air infiltration model-long-term field test validation. *Semi-Annu Meet ASHRAE* 1982: 1: 1351–1372.

ICRP. *2005 Recommendations of the International Commission on Radiological Protection: Summary of the Recommendations (Draft)*. International Commission on Radiological Protection (ICRP), Stockholm, 2005.

Ingersoll J.G. A survey of radionuclide contents and radon emanation rates in building materials used in the U.S. *Health Phys* 1983: 45(2): 363–368.

Khan A.J., Prasad R., and Tyagi R.K. Measurement of radon exhalation rate from some building materials. *Nucl Tracks Radiat Meas* 1992: 20(4): 609–610.

Kobeissi M.A., El Samad O., Zahraman K., Milky S., Bahsoun F., and Abumurad K.M. Natural radioactivity measurements in building materials in Southern Lebanon. *J Environ Radioact* 2008: 99: 1279–1288.

Lee S.C., Kim C.K., Lee D.M., and Kang H.D. Natural radionuclides contents and radon exhalation rates in building materials used in South Korea. *Radiat Prot Dosimetry* 2001: 94(3): 269–274.

MacIntosh D., Minegishi T., Kaufman M., Baker B., Allen J., Levy J., and Myatt T. The benefits of whole-house in-duct air cleaning in reducing exposures to fine particulate matter of outdoor origin: a modeling analysis. *J Expo Sci Environ Epidemiol* 2009, advance online publication, 25 March 2009; doi:10.1038/jes.2009.16.

Maged A.F., and Ashraf F.A. Radon exhalation rate of some building materials used in Egypt. *Environ Geochem Health* 2005: 27(5-6): 485–489.

Marcinowski F., Lucas R.M., and Yeager W.M. National and regional distributions of airborne radon concentrations in US homes. *Health Phys* 1994: 66(6): 699–706.

Mustonen R. Natural radioactivity in and radon exhalation from Finnish building materials. *Health Phys* 1984: 46(6): 1195–1203.

Myatt T.A., Minegishi T., Allen J.G., and Macintosh D.L. Control of asthma triggers in indoor air with air cleaners: a modeling analysis. *Environ Health* 2008: 7: 43.

Myatt T.A., Allen J.G., Minegishi T., McCarthy W.B., and MacIntosh D.L. Assessing exposure to radiation from granite countertops. *J Expo Sci Environ Epidemiol* 2009 (Submitted).

NCRP. *Radiation Exposure of the US Population from Consumer Products and Miscellaneous Sources*. National Council on Radiation Protection and Measurements (NCRP), Bethesda, MD, 1987a.

NCRP. *Exposure of the Population in the United States and Canada from Natural Background Radiation*. National Council on Radiation Protection and Measurements (NCRP), Bethesda, MD, 1987b.

NCRP. *Limitation of Exposure to Ionizing Radiation*. National Council on Radiation Protection and Measurements (NCRP), Bethesda, MD, 1993.

Ngachin M., Garavaglia M., Giovani C., Nourreddine A., Kwato Njock M.G., Scruzzi E., and Lagos L. (226)Ra, (232)Th and (40)K contents and radon exhalation rate from materials used for construction and decoration in Cameroon. *J Radiol Protect* 2008: 28(3): 369–378.

Osmanlioglu A.E. Natural radioactivity and evaluation of effective dose equivalent of granites in Turkey. *Radiat Prot Dosimetry* 2006: 121(3): 325–329.

Palmiter L, and Brown I *Northwest Residential Infiltration Survey: Analysis and Results*. Ecotope for Washington State Energy Office, Seattle, WA, USA, 1989, 52.

Parker GB, McSorley M, and Harris J The Northwest residential infiltration survey: a field study of ventilation in new homes in the Pacific Northwest. In: Sherman M.H. (Ed.). *Air Change Rate and Airtightness in Buildings, ASTM STP 1067*. ASTM International, 1990: Richmond, WA, pp. 93–103.

Petropoulos N.P., Anagnostakis M.J., and Simopoulos S.E. Photon attenuation, natural radioactivity content and radon exhalation rate of building materials. *J Environ Radioact* 2002: 61(3): 257–269.

Sahoo B.K., Nathwani D., Eappen K.P., Ramachandran T.V., Gaware J.J., and Mayya Y.S. Estimation of radon emanation factor in Indian building materials. *Radiat Meas* 2007: 42: 1422–1425.

Material may be protected by copyright law (Title 17, U.S. Code)

Singh H., Singh J., Singh S., and Bajwa B.S. Radon exhalation rate and uranium estimation study of some soil and rock samples from Tusham ring complex, India using SSNTD technique. *Radiat Meas* 2008: 43(Supplement 1): S459–S462.

Sonkawade R.G., Kant K., Muralithar S., Kumar R., and Ramola R.C. Natural radioactivity in common building construction and radiation shielding materials. *Atmos Environ* 2008: 42: 2254–2259.

Stoulos S., Manolopoulou M., and Papastefanou C. Assessment of natural radiation exposure and radon exhalation from building materials in Greece. *J Environ Radioact* 2003: 69(3): 225–240.

Stranden E. Building materials as a source of indoor radon, Chapter 3. In: Nazaroff W.W, and Nero A.V. (Eds.). *Radon and Its Decay Products in Indoor Air*. John Wiley & Sons, New York, NY, 1988.

Sundar S.B., Ajoy K.C., Dhanasekaran A., Gajendiran V., and Santhanam R. Measurement of radon exhalation rate from Indian granite tiles. *2003 Int Radon Symp* 2003: II: 78–103.

US EPA. *Radon Mitigation Standards*. US Environmental Protection Agency, 1993: Washington, DC.

Walton G., and Dols W.S. *CONTAM 2.1 Supplemental user guide and program documentation*. National Institute of Standards and Technology, Gaithersberg, MD, 2003.

Material may be protected by copyright law (Title 17, U.S. Code)